Fast impurity solver based on Gutzwiller variational approach

Jia Ning Zhuang, Lei Wang, Zhong Fang, and Xi Dai
Institute of Physics, Chinese Academy of Sciences, Beijing 100190, People's Republic of China
(Received 18 October 2008; revised manuscript received 19 March 2009; published 23 April 2009)

A fast impurity solver for the dynamical mean-field theory (DMFT) named two-mode approximation is proposed based on the Gutzwiller variational approach, which captures the main features of both the coherent and incoherent motion of the electrons. The solver works with real frequency at zero temperature and it provides directly the spectral function of the electrons. It can be easily generalized to multiorbital impurity problems with general on-site interactions, which makes it very useful in local-density approximation plus DMFT. Benchmarks on one- and two-band Hubbard models are presented, and the results agree well with those of exact diagonalization. Lastly a few cartoonlike five-band results are presented, showing that the present solver is really capable of dealing with multiband systems.

DOI: 10.1103/PhysRevB.79.165114 PACS number(s): 71.27.+a, 71.10.Fd, 71.20.Be

I. INTRODUCTION

The accurate calculation of the electronic structure of materials starting from first principles is a challenging problem in condensed-matter science. The local-density approximation (LDA) based on density-functional theory (DFT) is a widely used *ab initio* method,[1] which has been successfully applied to study the properties of simple metals and semiconductors, as well as the band insulators. However, it cannot be applied to those materials containing partially filled narrow bands from d or f shells because of the so-called strong correlation effect.

In LDA the delocalized nature rather than the localized feature of the electronic state is emphasized, so it is more suitable to describe those wide energy bands contributed by the electrons from outer shells. While for the electrons from those unclosed inner shells like $3d$ or $5f$ shells, some atomic features such as the multiplet structure remain, which are poorly described by LDA. Therefore for those strongly correlated materials, we have to implement LDA with some many-body techniques which can deal with the strong correlation effect and capture most of the atomic features.

One notable example of the first-principle schemes is the LDA+U method,[2] which can successfully describe many interesting effects such as spin, orbital, and charge ordering in transition-metal compounds.[3] Although LDA+U can capture the static orbital and spin-dependent physics quite well, it still cannot consider the dynamical correlation effect, which causes lots of interesting phenomena like Mott transition.[4–6]

Another attempt is to use Gutzwiller variational approach[7,8] to take into account the correlation effect (LDA+G), which has been successfully applied to many systems.[9–11] LDA+G treatment has its advantage in describing ground state and low-energy excited states, but it cannot properly describe the finite temperature and dynamical properties due to the lack of high-energy excited states. In order to capture the overall features of a correlated materials, more sophisticated approaches are needed.

During the past twenty years, the dynamical mean-field theory (DMFT) (Ref. 12) has been quickly developed to be a powerful method to solve the strongly correlated models on the lattice. DMFT maps the lattice models to the corresponding quantum impurity models subject to self-consistency conditions. Unlike the normal static mean-field approaches, DMFT keeps the full local dynamics induced by the local interaction. DMFT has been successfully applied to various of correlation problems, such as the Mott transition in Hubbard model,[13,14] the pseudogap behavior in high-T_c cuprates,[15] and the heavy fermion system.[16,17] Since DMFT can capture quite accurately the correlation features induced by the on-site Coulomb interaction and LDA can take care of the periodic potential as well as the long-range part of the Coulomb interaction, the combination of the two methods should be a very useful scheme for the first-principles calculation of the correlation materials. In the past twenty years, LDA+DMFT has been developed very quickly and successfully applied to many systems,[18] see Refs. 19–22 for reviews of the recent developments and applications.

In LDA+DMFT, one encounters the problem of how to efficiently solve quantum impurity problems with self-consistently determined heat bath. A fast impurity solver can be regarded as the *engine* of DMFT, which determines the efficiency and accuracy of DMFT. Many impurity solvers have been developed in the past twenty years, which can be divided into analytical methods and numerical methods. The analytical methods include equation of motion (EOM) method,[23] Hubbard-I approximation,[24,25] iterative perturbation theory (IPT),[26,27] the noncrossing approximation (NCA),[28] and the fluctuation exchange approximation (FLEX).[29] The numerical methods include exact diagonalization (ED),[30] Hirsch-Fye Quantum Monte Carlo methods,[31,32] and the numerical renormalization group (NRG).[33] Most recently a powerful continuous-time quantum Monte Carlo (CTQMC) solver[34,35] has also been developed and applied to several realistic materials.[36,37]

All these impurity solvers have their own advantages and the limitations as well. Since most of the novel quantum phenomena in condensed-matter physics happen in very low temperature, it is always very important for us to study the low-temperature properties of the correlated materials using LDA+DMFT. Up to now, the impurity solvers which can work at extremely low temperature are ED, IPT, and NRG. Among them, IPT can only apply to the single-band system; ED and NRG are numerically quite heavy for a general multiband system. Therefore it is very useful to develop an

impurity solver working at zero temperature, which satisfies the following criteria: (i) It can capture both the low-energy quasiparticle physics and the high-energy Hubbard bands; (ii) it works with real frequency and gives the real time dynamical properties directly; (iii) it is easy to be generalized to realistic multiband systems.

Here we propose a fast impurity solver based on Gutzwiller variational approach[9] which has the above three advantages. Gutzwiller variational wave function associated with Gutzwiller approximation (GA) was first proposed to deal with lattice problems such as the Hubbard model and the periodical Anderson model.[38,39] In the present paper, we apply a generalized Gutzwiller method called two-mode approximation (TMA) to calculate the Green's function for a quantum impurity model generated by DMFT. TMA is first proposed in Ref. 40 to calculate the spectral function for the lattice mode. Here we generalize it to the quantum impurity problem and make it a useful impurity solver for DMFT.

In TMA three different types of variational wave functions are constructed for the ground states, low-energy quasiparticle states, and high-energy excited state. All the variational parameters appearing in different wave functions are determined by minimizing the ground-state energy, based on which we can obtain the electronic spectral functions over the full frequency range. The computational time is mainly determined by the minimization of the ground-state energy and is similar with the previous study on lattice problem,[41] which can be easily done even on a single PC. This makes the present approach a fast general solver for LDA+DMFT studies.

The paper is organized as follows. In Sec. II we give the derivation of the method and prove that the sum rule for the electronic spectral function is satisfied. In Sec. III we benchmark the present impurity solver on the two-band Hubbard model with DMFT+ED. Finally a summary and the conclusions are made in Sec. IV.

II. DERIVATION OF THE METHOD

A. Gutzwiller ground state

Let us first consider the following multiorbital impurity Hamiltonian:

$$\hat{H}_{\mathrm{imp}} = \hat{H}_{\mathrm{band}} + \hat{H}_{\mathrm{local}} + \hat{H}_V,$$

$$\hat{H}_{\mathrm{band}} = \sum_{k\sigma} \epsilon_{k\sigma} \hat{c}^{+}_{k\sigma} \hat{c}_{k\sigma},$$

$$\hat{H}_{\mathrm{local}} = \sum_{\sigma,\sigma'} U_{\sigma\sigma'} \hat{n}_{f\sigma} \hat{n}_{f\sigma'} + \sum_{\sigma} \varepsilon_{\sigma} \hat{n}_{f\sigma},$$

$$\hat{H}_V = \sum_{k\sigma} V_{k\sigma} (\hat{c}^{+}_{k\sigma} \hat{f}_{\sigma} + \mathrm{H.c.}),$$

where k denotes the energy levels in the bath and σ is the joint index for orbital and spin. In Gutzwiller variational approach, the ground state of the above Hamiltonian can be written as

$$|\Psi\rangle = \hat{P}|0\rangle, \tag{1}$$

where $\hat{P}$ is the Gutzwiller projector and $|0\rangle$ is a single Slater-determinant-like wave function. Both of $\hat{P}$ and $|0\rangle$ will be determined by minimizing the ground-state energy. Following Ref. 9 the Gutzwiller projector can be written in terms of the projection operators of the atomic eigenstates as

$$\hat{P} = \sum_{\Gamma} \frac{\sqrt{m_{\Gamma}}}{\sqrt{m^0_{\Gamma}}} \hat{m}_{\Gamma}. \tag{2}$$

In Eq. (2), the operator $\hat{m}_{\Gamma} \equiv |\Gamma\rangle\langle\Gamma|$ is the projector to the eigenstates $|\Gamma\rangle$ of the atomic Hamiltonian $\hat{H}_{\mathrm{local}}$, and m_{Γ} are the variational parameters introduced in the Gutzwiller theory. Note that if $\hat{H}_{\mathrm{local}}$ only contains density-density interactions, the atomic eigenstates are known as the following Fock states:[9]

$$\Gamma \in \{\varnothing;(1),\ldots,(2N);(1,2),(2,3),\ldots(2N-1,2N);\ldots(1,\ldots,2N)\}, \tag{3}$$

where N is the number of orbitals. m^0_{Γ} is defined as

$$m^0_{\Gamma} \equiv \langle 0|\hat{m}_{\Gamma}|0\rangle. \tag{4}$$

Using the operator equalities

$$\hat{m}_{\Gamma} = \prod_{\sigma\in\Gamma} \hat{n}_{f\sigma} \prod_{\sigma\bar{\in}\Gamma} (1-\hat{n}_{f\sigma}), \tag{5}$$

$$\hat{n}_{f\sigma} = \sum_{\Gamma\ni\sigma} \hat{m}_{\Gamma} \tag{6}$$

with the definition $n^0_{f\sigma} \equiv \langle 0|\hat{n}_{f\sigma}|0\rangle$ and $n_{f\sigma} \equiv \langle\Psi|\hat{n}_{f\sigma}|\Psi\rangle$, one can prove that $m^0_{\Gamma} = \prod_{\sigma\in\Gamma} n^0_{f\sigma} \prod_{\sigma\bar{\in}\Gamma} (1-n^0_{f\sigma})$, $n^0_{f\sigma} = \Sigma_{\Gamma\ni\sigma} m^0_{\Gamma}$, and $n_{f\sigma} = \Sigma_{\Gamma\ni\sigma} m_{\Gamma}$. We would emphasize the fact that $n^0_{f\sigma} = n_{f\sigma}$ for Gutzwiller type wave functions with pure density-density interaction, which greatly simplifies the computation.[9,10] Therefore the Gutzwiller ground-state energy of this impurity model reads

$$E_g = \frac{\langle 0|\hat{P}\hat{H}_{\mathrm{imp}}\hat{P}|0\rangle}{\langle 0|\hat{P}^2|0\rangle}. \tag{7}$$

The denominator in the above equation can be expressed as

$$\langle 0|\hat{P}^2|0\rangle = \sum_{\Gamma} m_{\Gamma} = 1,$$

while the numerator can be calculated by decomposing the projectors as in Eq. (5) and applying the Wick's theorem.[42] Finally we obtain the ground-state energy as

$$E_g = \sum_{k\sigma} \epsilon_{k\sigma} \langle 0|\hat{c}^{+}_{k\sigma}\hat{c}_{k\sigma}|0\rangle + \sum_{\Gamma} E_{\Gamma} m_{\Gamma} + \sum_{k\sigma} z_{\sigma} V_{k\sigma} \langle 0|\hat{c}^{+}_{k\sigma}\hat{f}_{\sigma} + \mathrm{H.c.}|0\rangle$$

with

$$z_\sigma = \sum_{\Gamma \ni \sigma, \Gamma' = \Gamma \setminus \sigma} \frac{\sqrt{m_\Gamma m_{\Gamma'}}}{\sqrt{n^0_{f\sigma}(1-n^0_{f\sigma})}}.$$

The ground-state wave function $|\Psi\rangle$ can be obtained by minimizing the above energy functional with respect to the m_Γ and noninteracting wave function $|0\rangle$,[9,10] along with the following constraints:

$$\sum_\Gamma m_\Gamma = 1, \tag{8}$$

$$n_{f\sigma} = \sum_{\Gamma \ni \sigma} m_\Gamma. \tag{9}$$

B. Zero-temperature Green's function

For the impurity Hamiltonian Eq. (1), the retarded Green's function for the electrons on the impurity site reads

$$G^{\rm imp}_\sigma(\omega + i\eta) = \sum_n \frac{\langle\Psi|\hat{f}_\sigma|n\rangle\langle n|\hat{f}^\dagger_\sigma|\Psi\rangle}{\omega + i\eta - E_n + E_g} + \sum_m \frac{\langle\Psi|\hat{f}^\dagger_\sigma|m\rangle\langle m|\hat{f}_\sigma|\Psi\rangle}{\omega + i\eta + E_m - E_g}, \tag{10}$$

where $|\Psi\rangle$ is the ground state of $\hat{H}_{\rm imp}$ with the eigenenergy E_g and $|n\rangle$ ($|m\rangle$) are the eigenstates of $\hat{H}_{\rm imp}$ with one more (less) electron than the ground state. E_n and E_m are the corresponding eigenvalues. The above expression is exact if the summation of n and m includes all the eigenstates. In the present paper, we apply TMA to solve the quantum impurity problem, in which we limit the above summation in a truncated Hilbert space formed by finite number of excited states over the Gutzwiller variational ground state.[40,43] In order to capture the basic feature of the electronic spectral function efficiently, we have to include two types of excited states in TMA, namely, the quasiparticle excitations which give the right Fermi-liquid behavior in the low-energy and the high-energy excited states, which are responsible for the Hubbard bands or the atomic multiplet features. The former are called quasiparticle states and the latter are called bare-particle states in the present paper.[40] The ansatz for the excited states are the following:

$$|+k\sigma\rangle = \hat{c}^\dagger_{k\sigma}\hat{P}|0\rangle,$$

$$|UHB\rangle = \hat{f}^\dagger_\sigma\hat{P}|0\rangle,$$

$$|QE\rangle = \hat{P}\hat{f}^\dagger_\sigma|0\rangle,$$

$$|-k\sigma\rangle = \hat{c}_{k\sigma}\hat{P}|0\rangle,$$

$$|LHB\rangle = \hat{f}_\sigma\hat{P}|0\rangle,$$

$$|QH\rangle = \hat{P}\hat{f}_\sigma|0\rangle,$$

where $|QE\rangle$ ($|QH\rangle$) are the quasiparticle (quasihole) states, $|UHB\rangle$ ($|LHB\rangle$) are the bare-particle (bare-hole) states, and $|+-k\sigma\rangle$ represent the excitations in the bath.

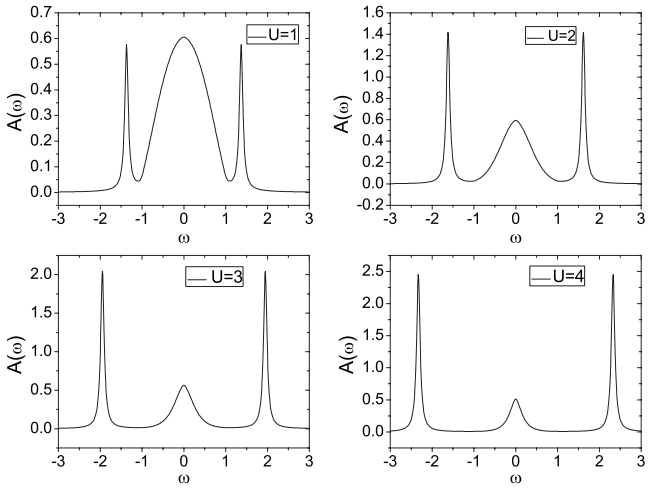

FIG. 1. The spectral function of electrons on the impurity site for an single orbital impurity model with different U and semicircular density of states in the bath.

The excited states listed above are neither orthogonal nor normalized; thus we have to calculate the overlaps $\mathcal{O}_{\alpha\beta} \equiv \langle\alpha|\beta\rangle$ and the matrix elements of the Hamiltonian $\mathcal{H}_{\alpha\beta} \equiv \langle\alpha|\hat{H}|\beta\rangle$ in this truncated Hilbert space. This procedure could be easily done by applying Wick's theorem. We list all the necessary matrix elements and overlaps in the Appendix.

In order to evaluate the Green's function using expression (10), we have to first obtain the eigenstates and eigenvalues by solving the following generalized eigenequation in the truncated Hilbert space:

$$\mathcal{H}|l\rangle = E_l\mathcal{O}|l\rangle.$$

Therefore $|l\rangle$ form a complete basis for the truncated Hilbert space and the completeness condition $\Sigma_l|l\rangle\langle l| = 1$ is satisfied within the truncated Hilbert space. Since both the states $\hat{f}^\dagger_\sigma\hat{P}|0\rangle$ and $\hat{f}_\sigma\hat{P}|0\rangle$ are fully contained in the Hilbert space, it is easy to prove that

$$\left(-\frac{1}{\pi}\right){\rm Im}[G^{\rm imp}_\sigma(\omega + i\eta)] = \langle\Psi|\hat{f}_\sigma\hat{f}^\dagger_\sigma + \hat{f}^\dagger_\sigma\hat{f}_\sigma|\Psi\rangle = 1,$$

which is the sum rule of the impurity Green's function.

III. BENCHMARK

A. Impurity spectral function

First of all we check the spectral function obtained by TMA for a single orbital impurity model with particle-hole symmetry. The density of states for the heat bath is chosen to be the semicircle with the half width $D=1$ and we discrete the bath parameter for the number of k number is $N_k=99$ for each orbital. The spectral functions for the electron on the impurity site with different Hubbard interaction U are shown in Fig. 1.

From Fig. 1 we find that the spectral function contains three parts: the quasiparticle peak and two Hubbard bands. With the increment of U, the spectral weight transfers from the low-energy quasiparticle part to the Hubbard bands. Also

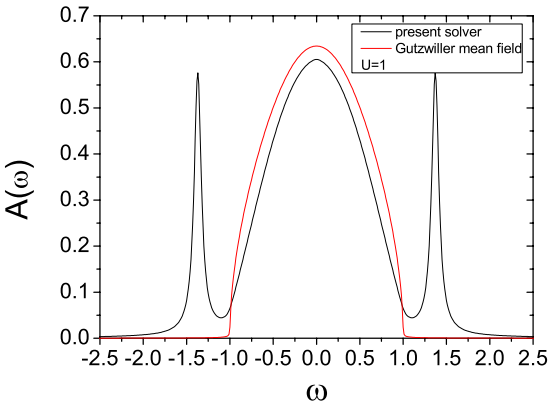

FIG. 2. (Color online) The spectral function of electrons on the impurity site for an single orbital impurity model obtained by TMA and GA lattice with $U=1$.

in large U limit, the distance between two Hubbard bands approaches U. All these features are consistent with the previous studies on the symmetric Anderson impurity model.[44] In Fig. 2, we compare the spectral function for an Anderson impurity model obtained by TMA with that by the normal GA (Refs. 7 and 9) for the lattice model, which only contains the quasiparticle part as

$$G_{\mathrm{imp}}^{\mathrm{GWMF}}(\omega+i\eta)=\frac{z^2}{\omega+i\eta+\tilde{\mu}-z^2\Delta(\omega+i\eta)}. \qquad (11)$$

Compared with normal Gutzwiller approximation (GA lattice), it is very clear that TMA can reproduce very nicely the low-energy quasiparticle part with slightly smaller spectral weight. Therefore the current solver can be viewed as the normal Gutzwiller approximation implemented with the Hubbard bands in the high-energy part of the electronic spectral functions describing the atomic features.

B. Used as the impurity solver in DMFT

The present impurity solver can be used in the dynamical mean-field theory to study the lattice models. In this paper we have studied both the single-band and two-band Hubbard model at paramagnetic phase with arbitrary fillings.

1. Single-band Hubbard model

We start with the single-band Hubbard model on the Bethe lattice with half bandwidth $D=1$. First we check the half-filling case. We show the spectral functions with the increment of U in Fig. 3, from which we see that the height of quasiparticle peak changes little before Mott transition, but the integral of the quasiparticle peak reduces as U increases.

We show the results for the systems away from half filling in Fig. 4.With the increment of filling factor from $N_{\mathrm{tot}}=0.2$ to half filling $N_{\mathrm{tot}}=1.0$, the spectral weight continuously transfers from the low-energy quasiparticle part to the high-energy Hubbard bands, which is consistent with the common understanding that the strong correlation effect is less pronounced when the system is doped away from half filling.

In Fig. 5, we quantitatively compare the density of states (DOS) obtained by DMFT+TMA with that by DMFT+ED.

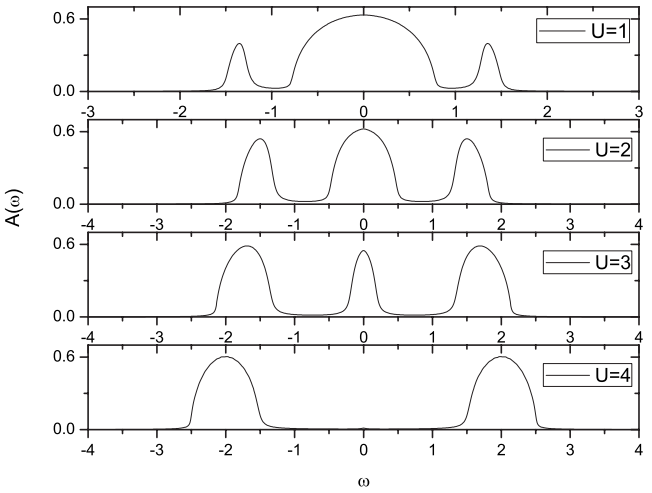

FIG. 3. The density of states (DOS) obtained by DMFT+TMA for single-band Hubbard model on Bethe lattice at half filling.

We find quite good agreement between them for both the half-filling and non-half-filling cases. However, we also find two disagreements. Compared with the DMFT+ED results, the total spectral weight of the quasiparticle part is overestimated while the width of the Hubbard bands is underestimated by DMFT+TMA.

The spectral functions have also been checked in challenging parameter regimes. For example, Fig. 6 shows that DMFT+TMA allows resolving in-gap states for a very weakly doped Mott insulator. Our results show that if one dopes holes into a Mott insulator, the spectral weight appears in the middle of the Mott gap, which is consistent with many previous DMFT studies.[12]

We have also calculated the quasiparticle weight z, which is a characteristic quantity describing the strength of the correlation effect and is defined as

$$z_\sigma=\left(1-\frac{\partial\,\mathrm{Re}\left[\sum_\sigma(\omega+i\eta)\right]}{\partial\omega}\right)^{-1}\Bigg|_{\omega=0}. \qquad (12)$$

In Fig. 7 we show quasiparticle weight obtained by DMFT+TMA as the function of U for different filling factors. In the half-filling case, the value of z decreases as the increment of U until the critical U_c for the Mott transition. As shown in Fig. 7, U_c obtained by DMFT+TMA is around 3.6, which is bigger than $U_{c2}=2.9$ obtained by DMFT+ED.

In Fig. 8, we compare the z factors obtained by DMFT+TMA, Gutzwiller approximation on the lattice model (lattice GA), and DMFT+ED. As discussed in Refs. 10 and 40 we can only obtain the ground-state energy quite accurately by lattice GA, but not for the z factor. The reason is quite obvious that in the lattice GA only the low-energy quasiparticle states in Eq. (10) can be considered, which limits the accuracy of z factor. While in TMA, we first apply the DMFT scheme to treat the intersite correlation on a mean-field level, which is in principle similar with GA. Then in solving the effective impurity model, we enlarge the variational space by including more excited states, which gives us

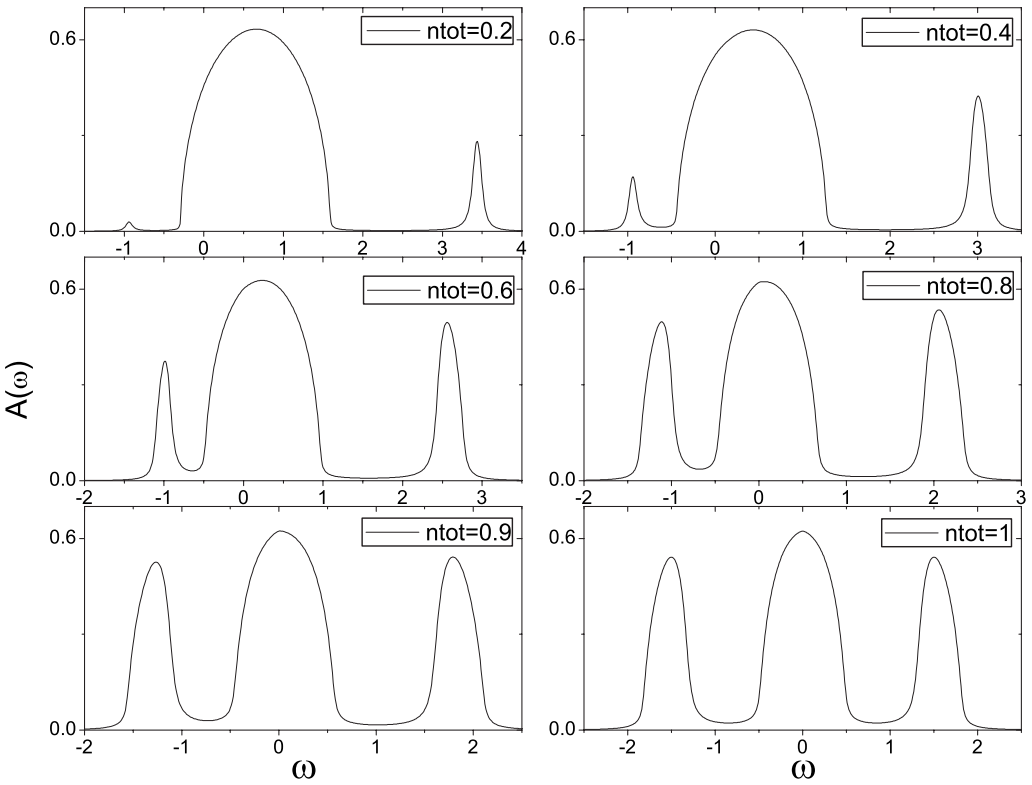

FIG. 4. The density of states (DOS) obtained by DMFT+TMA of single-band Hubbard model under $U=2$ with different fillings.

more accurate description of the low-energy excited states and successfully reduces the disagreement in z factor with DMFT+ED results as shown in Fig. 8.

2. Two-band Hubbard model on the Bethe lattice

The situation becomes more complicated when we consider two-band models. We start with the simplest case that the two bands are degenerate with half bandwidth $D_1=D_2=1$ and the local part of the Hamiltonian has SU(4) symmetry, which can be written as

$$\hat{H}_{\text{at}} = U\sum_{b} \hat{n}_{b,\uparrow}\hat{n}_{b,\downarrow} + U\sum_{\sigma,\sigma'} \hat{n}_{1,\sigma}\hat{n}_{2,\sigma'}. \tag{13}$$

We first show the quasiparticle weight obtained by DMFT+TMA versus U at different filling factors in Fig. 9 together with that from DMFT+ED and lattice GA in Fig. 10.

The Mott transition at integer fillings can be observed with U_c slightly larger than the DMFT+ED results. From Fig. 9 we see that $U_c=4.6$ for $N_{\text{tot}}=1$ and $U_c=5.0$ for $N_{\text{tot}}=2$. As shown in Fig. 10, the improvement of the quasiparticle weight against the lattice GA is quite dramatic, which

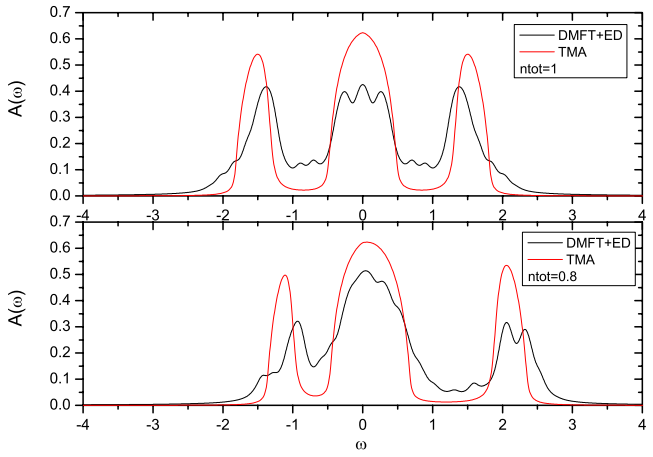

FIG. 5. (Color online) Comparison of the DOS obtained by DMFT+TMA and DMFT+ED for single-band Hubbard model with $U=2$.

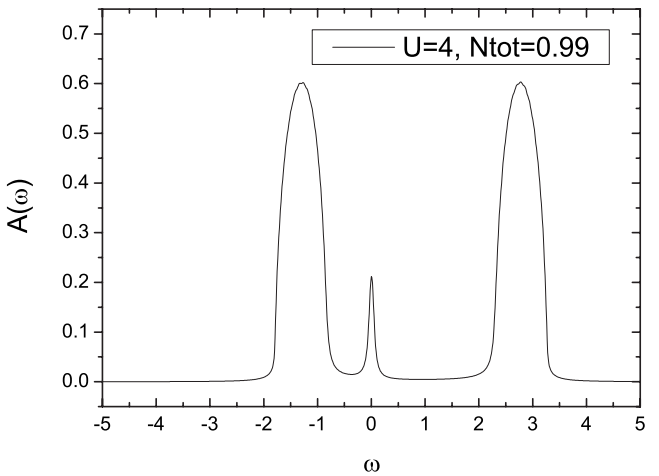

FIG. 6. The spectral function for in-gap states in weakly doped Mott insulator.

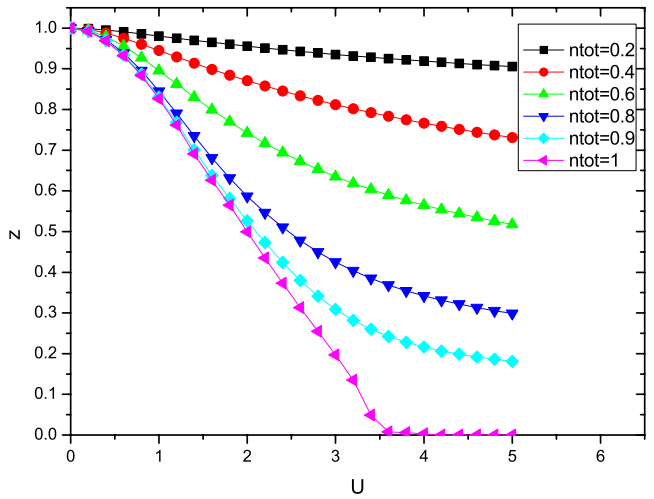

FIG. 7. (Color online) Quasiparticle weight z of single-band Hubbard model obtained by DMFT+TMA versus U at different fillings.

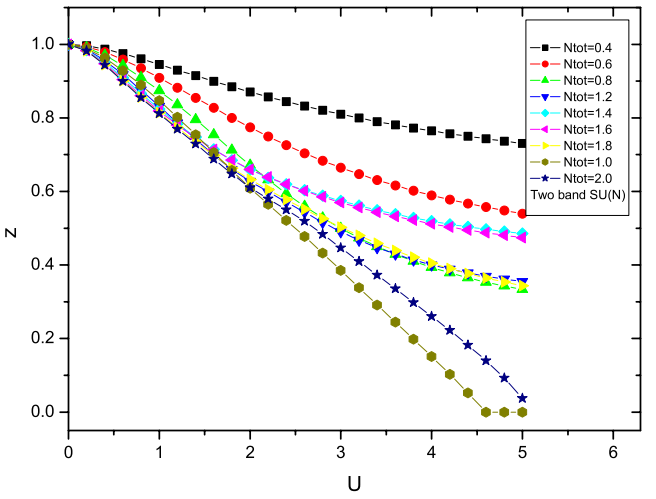

FIG. 9. (Color online) Quasiparticle weight z as the function of U for the two-band Hubbard model with SU(N) symmetry obtained by DMFT+TMA.

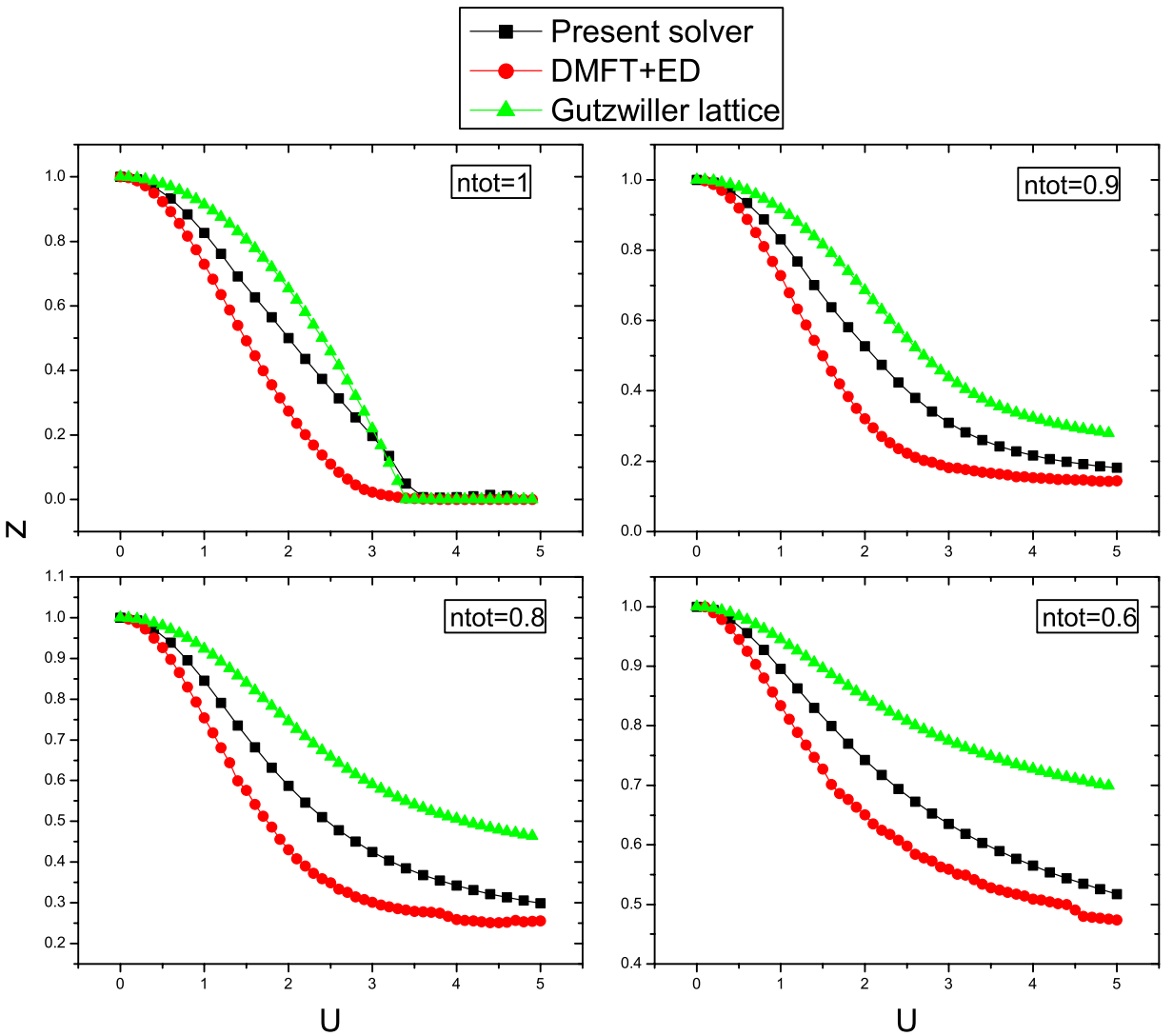

FIG. 8. (Color online) Comparison of Quasiparticle weight z for the single-band Hubbard model obtained by DMFT+TMA, GA lattice, and DMFT+ED.

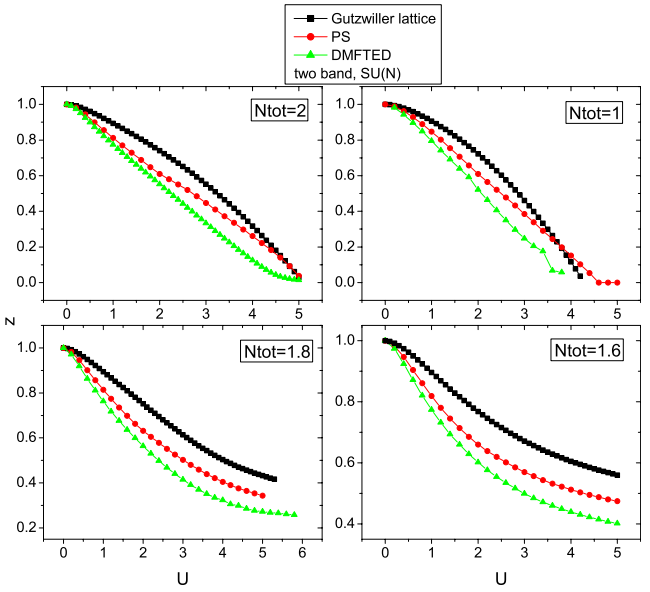

FIG. 10. (Color online) Comparison of quasiparticle weight z for the two-band Hubbard model with SU(N) symmetry at different fillings obtained by DMFT+TMA, GA lattice, and DMFT+ED.

indicates that even for the low-energy quasiparticle part the DMFT+TMA is better than applying the GA directly to the lattice model.

The behavior of z as the function of the filling factor for fixed $U=5.0$ is shown in Fig. 11, from which we can find that compared with lattice GA the results obtained by DMFT+TMA is much closer to DMFT+ED.

Next we take the Hund's coupling constant J into account. Then the local part of the Hamiltonian becomes

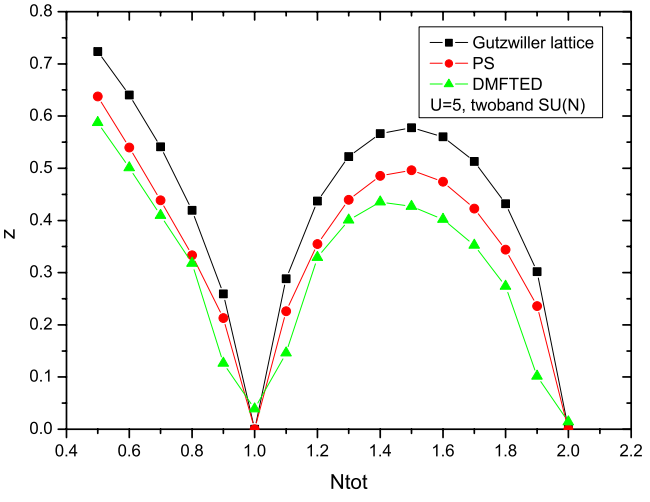

FIG. 11. (Color online) Comparison of quasiparticle weight z as the function of total number of particles for the two-band Hubbard model with SU(N) symmetry at $U=5$ obtained by DMFT+TMA, GA lattice, and DMFT+ED.

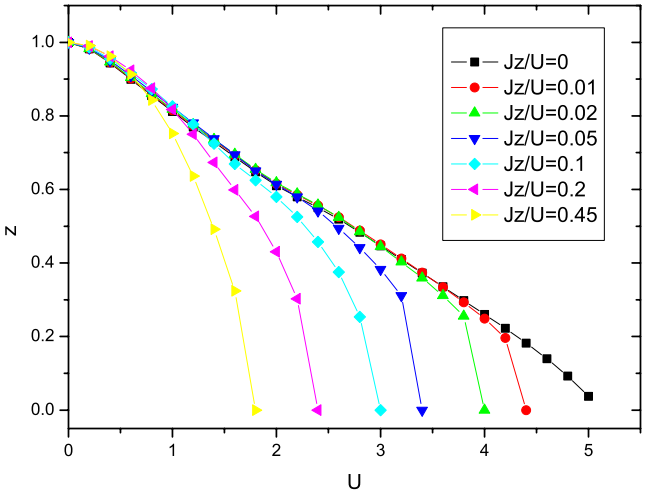

FIG. 12. (Color online) Quasiparticle weight z as the function of U for the two-degenerate-band Hubbard model with longitudinal Hund's coupling J_z obtained by DMFT+TMA with different J_z/U.

$$\hat{H}_{\text{at}} = U\sum_{b} \hat{n}_{b,\uparrow}\hat{n}_{b,\downarrow} + U'\sum_{\sigma,\sigma'} \hat{n}_{1,\sigma}\hat{n}_{2,\sigma'} - J\sum_{\sigma} \hat{n}_{1,\sigma}\hat{n}_{2,\sigma}$$
$$+ J\sum_{\sigma} \hat{c}^{+}_{1,\sigma}\hat{c}^{+}_{2,-\sigma}\hat{c}_{1.-\sigma}\hat{c}_{2,\sigma} + J(\hat{c}^{+}_{1,\uparrow}\hat{c}^{+}_{1,\downarrow}\hat{c}_{2.\downarrow}\hat{c}_{2,\uparrow}$$
$$+ \hat{c}^{+}_{2,\uparrow}\hat{c}^{+}_{2,\downarrow}\hat{c}_{1.\downarrow}\hat{c}_{1,\uparrow}). \quad (14)$$

We have the relation $U-U'=2J$ for system with cubic symmetry.[45] In the current study, we only keep the longitudinal part of the Hund's rule coupling and neglect the spin flip and pair hopping terms which correspond to the last two terms in the above equation, and use the symbol J_z to replace J,

$$\hat{H}_{\text{at}} = U\sum_{b} \hat{n}_{b,\uparrow}\hat{n}_{b,\downarrow} + U'\sum_{\sigma,\sigma'} \hat{n}_{1,\sigma}\hat{n}_{2,\sigma'} - J_z\sum_{\sigma} \hat{n}_{1,\sigma}\hat{n}_{2,\sigma}.$$

The results for the full rotational invariance interaction will be studied in detail and published elsewhere.

The quasiparticle weight obtained by DMFT+TMA as the function of U is shown in Fig. 12. We also compare the results with DMFT+ED in Fig. 13, from which we find that U_c obtained from DMFT+TMA is larger than that of DMFT+ED as for the single-band model.

In Fig. 12, we find that the Brinkman-Rice (BR) transition is continuous *only* at the point $J_z=0$ and first order like for all nonzero J_z, which is similar with the results in Ref. 9 obtained by rotational invariant Gutzwiller approximation. This similarity indicates that for degenerate multiband Hubbard model the basic feature of the BR transition does not strongly relies on the rotational invariant treatment of the interaction. Moreover, the similar discontinuity and the tendency that the critical U_c decreases as J_z/U increases is also obtained in Ref. 46, where the self-energy functional method is used.

However, for the nondegenerate multiband models, i.e., the two-band model with different band widths, the correct rotational invariant treatment is necessary to obtain some of the qualitative features like the orbital selective Mott transi-

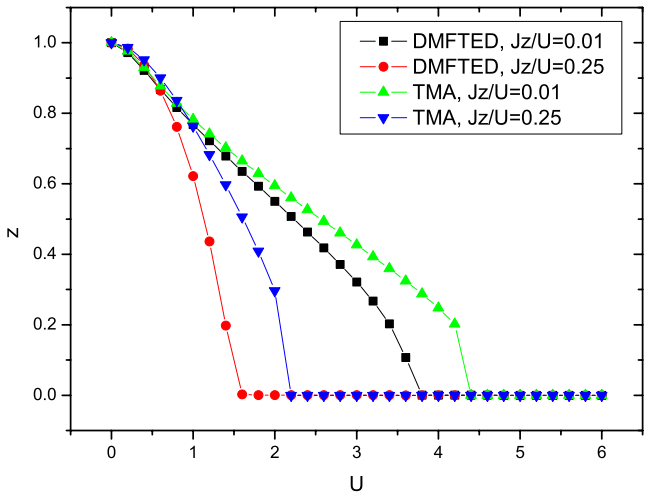

FIG. 13. (Color online) Comparison of quasiparticle weight z for the two-degenerate-band Hubbard model with longitudinal Hund's coupling J_z obtained by DMFT+TMA and DMFT+ED with different J_z/U.

tion (OSMT).[47] The detailed study for the OSMT using the rotational invariant TMA solver will be presented elsewhere. In the view of computational technique, we address that with the density-density interaction only, the occupation number for each band(spin) is still a good quantum number, and in this particular case, the computational time is linearly scaled with the number of the orbitals. While with more complicated interaction such as spin flip and pair hopping, the computation time will be exponentially scaled with the orbital degeneracy and further truncation will be needed.

Here we only give the results for an extreme case, where the band width difference of the two bands is very large. In Figs. 14 and 15, we represent the DOS as well as the quasiparticle weight as the functional of U with fixed $J_z/U=0.3$ and half bandwidth $D_1=1.0$ and $D_2=6.0$. Obviously in such extreme case, the system is in the orbital selective Mott phase which is consistent with Ref. 48.

3. Results of multiband Hubbard model

As it is mentioned above, the present solver of DMFT+TMA could be applied far beyond two-band Hubbard model. In this section we benchmark our impurity solver on multiband Hubbard model. As an example, for degenerate orbitals with SU(N) interactions at half filling on Bethe lattice with half bandwidth $D=2t=1$, we find that $U_c \approx 3.6, 5.0, 6.4, 7.9, 9.8$ for one-band, two-band, three-band, four-band, and five-band systems, respectively. The results is comparable with linearized DMFT by Potthoff[49] (see Fig. 16).

Typically, we have shown a spectral function for five-band degenerate band under SU(N) interaction with $U=4$ in

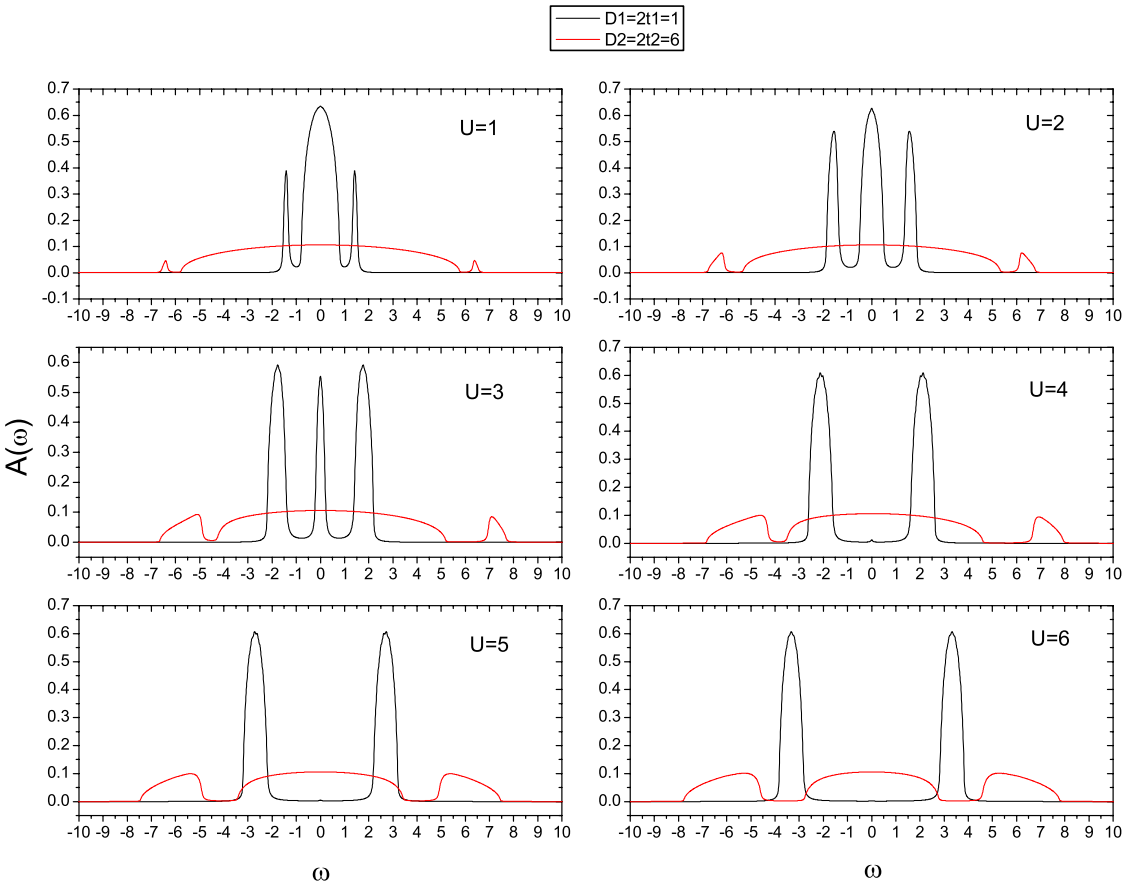

FIG. 14. (Color online) The spectral functions obtained by DMFT+TMA for two-nondegenerate-band Hubbard model with band width ratio 1:6 under different U with $J_z=0.3U$.

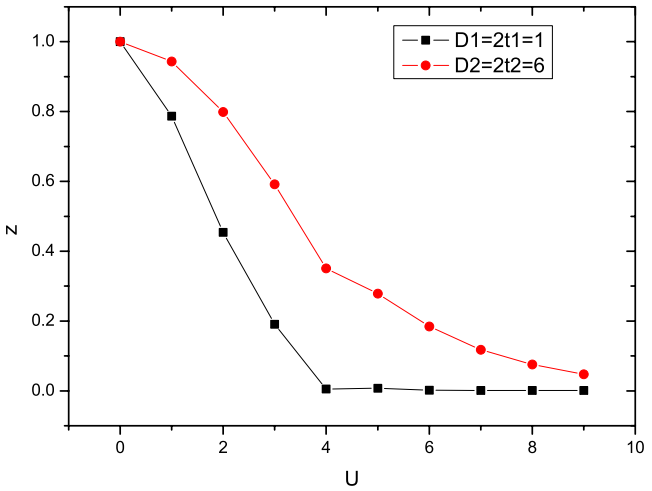

FIG. 15. (Color online) Quasiparticle weight z of different bands as the function of U for two-nondegenerate-band Hubbard model with band width ratio 1:6 under different U with $J_z=0.3U$.

Fig. 17. Meanwhile, Fig. 18 exhibits a nondegenerate band system with the interaction of $U=2$, $U'=1.2$, and $J_z=0.4$. The spectral functions have approved that the present solver of DMFT+TMA is promising and potential for multiband systems in authentic electron structure calculations.

IV. CONCLUSIONS

In this paper we present an impurity solver named two-mode approximation (TMA) for the multiorbital quantum impurity model generated by DMFT. By constructing the trial wave functions based on the Gutzwiller variational theory not only for the ground state but also the low-energy and high-energy excited states, we can obtain the spectral functions of the electrons on the impurity level with the satisfactory of the sum rule. Compared with other popular impurity solvers, TMA works with the real frequency and can obtain both the low-energy quasiparticle and high-energy Hubbard band behavior. In multiband system with density-density interactions, the computation time scales linearly with the system size. Moreover TMA can be generalized to treat the problem with quite general on-site interaction, which make it a good solver to be used in LDA+DMFT.

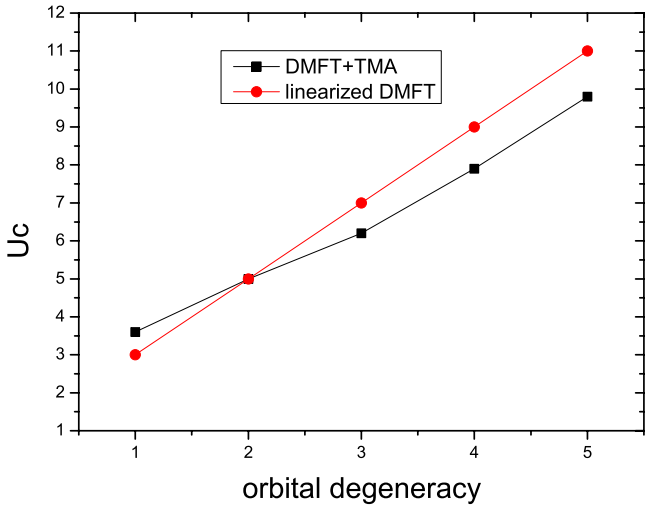

FIG. 16. (Color online) The critical U_c at paramagnetic phase on Bethe lattice of half bandwidth $t=0.5$ with SU(N) interactions as a function of orbital degeneracy given by DMFT+TMA compared with Gutzwiller analytical approach and linearized DMFT.

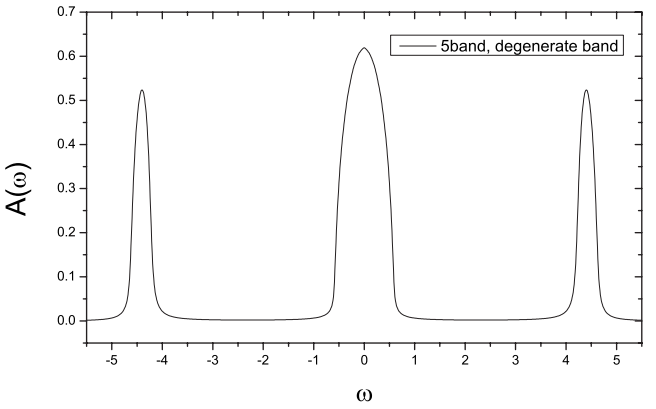

FIG. 17. The spectral function obtained by DMFT+TMA for five-degenerate band Hubbard model on Bethe lattice with bandwidth=1 and SU(N) interaction with U=4.

ACKNOWLEDGMENT

The authors would thank N. H. Tong, Q. M. Liu, X. Y. Deng, and Y. Wan for their helpful discussions. We acknowledge the support from NSF of China, and that from the 973 program of China (Grant No. 2007CB925000).

APPENDIX: OVERLAPS AND HAMILTONIAN ELEMENTS

1. Overlaps

We define

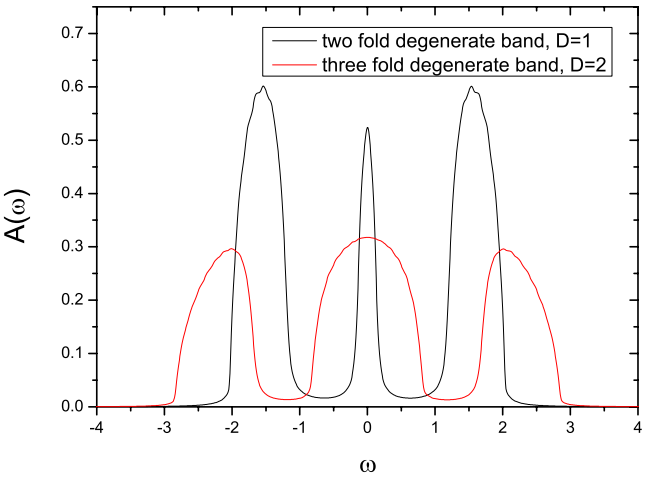

FIG. 18. (Color online) The spectral function obtained by DMFT+TMA for five-nondegenerate band Hubbard model on Bethe lattice with half-bandwidth=0.5,0.5,1,1,1 at $U=2$, $U'=1.2$, and $J_z=0.4$.

$$z_\sigma = \sum_{\Gamma \ni \sigma, \Gamma' = \Gamma \setminus \sigma} \frac{\sqrt{m_\Gamma m_{\Gamma'}}}{\sqrt{n^0_{f\sigma}(1-n^0_{f\sigma})}}.$$

The nonvanishing overlaps are

$$\langle + k_1\sigma | + k_2\sigma \rangle = \langle 0 | \hat{c}_{k_1\sigma} \hat{c}^+_{k_2\sigma} | 0 \rangle,$$

$$\langle + k\sigma | UHB \rangle = z_\sigma \langle 0 | \hat{c}_{k\sigma} \hat{f}^\dagger_\sigma | 0 \rangle,$$

$$\langle + k\sigma | QE \rangle = \langle 0 | \hat{c}_{k\sigma} \hat{f}^\dagger_\sigma | 0 \rangle,$$

$$\langle UHB | UHB \rangle = (1 - n^0_{f\sigma}),$$

$$\langle UHB | QE \rangle = z_\sigma (1 - n^0_{f\sigma}),$$

$$\langle QE | QE \rangle = (1 - n^0_{f\sigma}),$$

$$\langle - k_1\sigma | - k_2\sigma \rangle = \langle 0 | \hat{c}^+_{k_1\sigma} \hat{c}_{k_2\sigma} | 0 \rangle,$$

$$\langle - k\sigma | LHB \rangle = z_\sigma \langle 0 | \hat{c}^+_{k\sigma} \hat{f}_\sigma | 0 \rangle,$$

$$\langle - k\sigma | QH \rangle = \langle 0 | \hat{c}^+_{k\sigma} \hat{f}_\sigma | 0 \rangle,$$

$$\langle LHB | LHB \rangle = n^0_{f\sigma},$$

$$\langle LHB | QH \rangle = z_\sigma n^0_{f\sigma},$$

$$\langle LHB | LHB \rangle = n^0_{f\sigma}.$$

2. Hamiltonian Elements

The Hamiltonian elements are

$$\hat{H} = \hat{H}_{\text{band}} + \hat{H}_{\text{local}} + \hat{H}_V,$$

$$\hat{H}_{\text{band}} = \sum_{k\sigma} \epsilon_{k\sigma} \hat{c}^+_{k\sigma} \hat{c}_{k\sigma},$$

$$\hat{H}_{\text{local}} = \sum_\Gamma E_\Gamma \hat{m}_\Gamma + \sum_\sigma \varepsilon_\sigma \sum_{\Gamma \ni \sigma} \hat{m}_\Gamma,$$

$$\hat{H}_V = \sum_{k\sigma} V_{k\sigma} (\hat{c}^+_{k\sigma} \hat{f}_\sigma + \text{H.c.}).$$

a. H_{band}

We define

$$x_{\sigma\sigma'} = \sum_{\substack{\Gamma_2 \ni \sigma, \Gamma_2 \ni \sigma' \\ \Gamma_1 = \Gamma_2 \setminus \sigma'}} \frac{\sqrt{m_{\Gamma_1} m_{\Gamma_2}}}{n^0_{f\sigma} \sqrt{n^0_{f\sigma'}(1-n^0_{f\sigma'})}},$$

$$y_{\sigma\sigma'} = \sum_{\substack{\Gamma_1 \ni \sigma, \Gamma_1 \bar{\ni} \sigma' \\ \Gamma_2 = \Gamma_1 \cup \sigma' \setminus \sigma}} \frac{\sqrt{m_{\Gamma_1} m_{\Gamma_2}}}{\sqrt{n^0_{f\sigma}(1-n^0_{f\sigma}) n^0_{f\sigma'}(1-n^0_{f\sigma'})}},$$

$$w_{\sigma\sigma'} = \sum_{\substack{\Gamma_2 \bar{\ni} \sigma, \Gamma_2 \bar{\ni} \sigma' \\ \Gamma_1 = \Gamma_2 \cup \sigma \cup \sigma'}} \frac{\sqrt{m_{\Gamma_1} m_{\Gamma_2}}}{\sqrt{n^0_{f\sigma}(1-n^0_{f\sigma}) n^0_{f\sigma'}(1-n^0_{f\sigma'})}},$$

$$v_{\sigma\sigma'} = \sum_{\substack{\Gamma_1 \bar{\ni} \sigma, \Gamma_1 \bar{\ni} \sigma \\ \Gamma_2 = \Gamma_1 \cup \sigma'}} \frac{\sqrt{m_{\Gamma_1} m_{\Gamma_2}}}{(1-n^0_{f\sigma}) \sqrt{n^0_{f\sigma'}(1-n^0_{f\sigma'})}},$$

and

$$B^{++}_{\sigma\sigma'} = \sum_{\Gamma \ni \sigma, \Gamma \ni \sigma'} \frac{m_\Gamma}{n^0_{f\sigma} n^0_{f\sigma'}},$$

$$B^{+-}_{\sigma\sigma'} = \sum_{\Gamma \ni \sigma, \Gamma \bar{\ni} \sigma'} \frac{m_\Gamma}{n^0_{f\sigma}(1-n^0_{f\sigma'})},$$

$$B^{--}_{\sigma\sigma'} = \sum_{\Gamma \bar{\ni} \sigma, \Gamma \bar{\ni} \sigma'} \frac{m_\Gamma}{(1-n^0_{f\sigma})(1-n^0_{f\sigma'})}.$$

We will have

$$\begin{aligned}
\langle + k_1\sigma | \hat{H}_{\text{band}} | + k_2\sigma \rangle = \sum_{k'\sigma'} \epsilon_{k'\sigma'} [& \delta_{\sigma\sigma'} \langle 0 | \hat{c}_{k_1\sigma} \hat{c}^+_{k'\sigma} \hat{c}_{k'\sigma} \hat{c}^+_{k_2\sigma} | 0 \rangle \\
& + (1 - \delta_{\sigma\sigma'}) (B^{++}_{\sigma\sigma'} \langle 0 | \hat{c}_{k_1\sigma} \hat{c}^+_{k_2\sigma} \hat{f}^\dagger_\sigma \hat{f}_\sigma | 0 \rangle \\
& \times \langle 0 | \hat{c}^+_{k'\sigma'} \hat{c}_{k'\sigma'} \hat{f}^\dagger_{\sigma'} \hat{f}_{\sigma'} | 0 \rangle \\
& + B^{+-}_{\sigma\sigma'} \langle 0 | \hat{c}_{k_1\sigma} \hat{c}^+_{k_2\sigma} \hat{f}^\dagger_\sigma \hat{f}_\sigma | 0 \rangle \\
& \times \langle 0 | \hat{c}^+_{k'\sigma'} \hat{c}_{k'\sigma'} \hat{f}_{\sigma'} \hat{f}^\dagger_{\sigma'} | 0 \rangle \\
& + B^{+-}_{\sigma'\sigma} \langle 0 | \hat{c}_{k_1\sigma} \hat{c}^+_{k_2\sigma} \hat{f}_\sigma \hat{f}^\dagger_\sigma | 0 \rangle \\
& \times \langle 0 | \hat{c}^+_{k'\sigma'} \hat{c}_{k'\sigma'} \hat{f}^\dagger_{\sigma'} \hat{f}_{\sigma'} | 0 \rangle \\
& + B^{--}_{\sigma\sigma'} \langle 0 | \hat{c}_{k_1\sigma} \hat{c}^+_{k_2\sigma} \hat{f}_\sigma \hat{f}^\dagger_\sigma | 0 \rangle \\
& \times \langle 0 | \hat{c}^+_{k'\sigma'} \hat{c}_{k'\sigma'} \hat{f}_{\sigma'} \hat{f}^\dagger_{\sigma'} | 0 \rangle)],
\end{aligned}$$

$$\begin{aligned}
\langle + k\sigma | \hat{H}_{\text{band}} | UHB \rangle = \sum_{k'\sigma'} \epsilon_{k'\sigma'} [& \delta_{\sigma\sigma'} z_\sigma \langle 0 | \hat{c}_{k\sigma} \hat{c}^+_{k'\sigma} \hat{c}_{k'\sigma} \hat{f}^\dagger_\sigma | 0 \rangle \\
& + (1 - \delta_{\sigma\sigma'}) \langle 0 | \hat{c}_{k\sigma} \hat{f}^\dagger_\sigma | 0 \rangle \\
& \times (x_{\sigma'\sigma} \langle 0 | \hat{c}^+_{k'\sigma'} \hat{c}_{k'\sigma'} \hat{f}^\dagger_{\sigma'} \hat{f}_{\sigma'} | 0 \rangle \\
& + v_{\sigma'\sigma} \langle 0 | \hat{c}^+_{k'\sigma'} \hat{c}_{k'\sigma'} \hat{f}_{\sigma'} \hat{f}^\dagger_{\sigma'} | 0 \rangle)],
\end{aligned}$$

$$\begin{aligned}
\langle + k\sigma | \hat{H}_{\text{band}} | QE \rangle = \sum_{k'\sigma'} \epsilon_{k'\sigma'} [& \delta_{\sigma\sigma'} \langle 0 | \hat{c}_{k\sigma} \hat{c}^+_{k'\sigma} \hat{c}_{k'\sigma} \hat{f}^\dagger_\sigma | 0 \rangle \\
& + (1 - \delta_{\sigma\sigma'}) \langle 0 | \hat{c}_{k\sigma} \hat{f}^\dagger_\sigma | 0 \rangle \\
& \times (B^{++}_{\sigma\sigma'} \langle 0 | \hat{c}^+_{k'\sigma'} \hat{c}_{k'\sigma'} \hat{f}^\dagger_{\sigma'} \hat{f}_{\sigma'} | 0 \rangle
\end{aligned}$$

$$+ B^{+-}_{\sigma\sigma'}\langle 0|\hat{c}^{+}_{k'\sigma'}\hat{c}_{k'\sigma'}\hat{f}_{\sigma'}\hat{f}^{\dagger}_{\sigma'}|0\rangle)],$$

$$\langle UHB|\hat{H}_{\rm band}|UHB\rangle = \sum_{k'\sigma'}\epsilon_{k'\sigma'}[\delta_{\sigma\sigma'}\langle 0|\hat{f}_{\sigma}\hat{c}^{+}_{k'\sigma}\hat{c}_{k'\alpha}\hat{f}^{\dagger}_{\sigma}|0\rangle + (1-\delta_{\sigma\sigma'})(1-n^{0}_{f\sigma}) \times (B^{+-}_{\sigma'\sigma}\langle 0|\hat{c}^{+}_{k'\sigma'}\hat{c}_{k'\sigma'}\hat{f}^{\dagger}_{\sigma'}\hat{f}_{\sigma'}|0\rangle + B^{--}_{\sigma\sigma'}\langle 0|\hat{c}^{+}_{k'\sigma'}\hat{c}_{k'\sigma'}\hat{f}_{\sigma'}\hat{f}^{\dagger}_{\sigma'}|0\rangle) ,$$

$$\langle UHB|\hat{H}_{\rm band}|QE\rangle = \sum_{k'\sigma'}\epsilon_{k'\sigma'}[\delta_{\sigma\sigma'}z_{\sigma}\langle 0|\hat{f}_{\sigma}\hat{c}^{+}_{k'\sigma}\hat{c}_{k'\alpha}\hat{f}^{\dagger}_{\sigma}|0\rangle + (1-\delta_{\sigma\sigma'})(1-n^{0}_{f\sigma}) \times (x_{\sigma'\sigma}\langle 0|\hat{c}^{+}_{k'\sigma'}\hat{c}_{k'\sigma'}\hat{f}^{\dagger}_{\sigma'}\hat{f}_{\sigma'}|0\rangle + v_{\sigma'\sigma}\langle 0|\hat{c}^{+}_{k'\sigma'}\hat{c}_{k'\sigma'}\hat{f}_{\sigma'}\hat{f}^{\dagger}_{\sigma'}|0\rangle) ,$$

$$\langle QE|\hat{H}_{\rm band}|QE\rangle = \sum_{k'\sigma'}\epsilon_{k'\sigma'}[\delta_{\sigma\sigma'}\langle 0|\hat{f}_{\sigma}\hat{c}^{+}_{k'\sigma}\hat{c}_{k'\alpha}\hat{f}^{\dagger}_{\sigma}|0\rangle + (1-\delta_{\sigma\sigma'}) \times(1-n^{0}_{f\sigma})(B^{++}_{\sigma\sigma'}\langle 0|\hat{c}^{+}_{k'\sigma'}\hat{c}_{k'\sigma'}\hat{f}^{\dagger}_{\sigma'}\hat{f}_{\sigma'}|0\rangle + B^{+-}_{\sigma\sigma'}\langle 0|\hat{c}^{+}_{k'\sigma'}\hat{c}_{k'\sigma'}\hat{f}_{\sigma'}\hat{f}^{\dagger}_{\sigma'}|0\rangle) ,$$

$$\begin{aligned}\langle -k_1\sigma|\hat{H}_{\rm band}|-k_2\sigma\rangle &= \sum_{k'\sigma'}\epsilon_{k'\sigma'}[\delta_{\sigma\sigma'}\langle 0|\hat{c}^{+}_{k_1\sigma}\hat{c}^{+}_{k'\sigma}\hat{c}_{k'\sigma}\hat{c}_{k_2\sigma}|0\rangle + (1-\delta_{\sigma\sigma'}) \times(B^{++}_{\sigma\sigma'}\langle 0|\hat{c}^{+}_{k_1\sigma}\hat{c}_{k_2\alpha}\hat{f}^{\dagger}_{\alpha}\hat{f}_{\sigma}|0\rangle\langle 0|\hat{c}^{+}_{k'\sigma'}\hat{c}_{k'\sigma'}\hat{f}^{\dagger}_{\sigma'}\hat{f}_{\sigma'}|0\rangle \\ &+ B^{+-}_{\sigma\sigma'}\langle 0|\hat{c}^{+}_{k_1\sigma}\hat{c}_{k_2\alpha}\hat{f}^{\dagger}_{\alpha}\hat{f}_{\sigma}|0\rangle\langle 0|\hat{c}^{+}_{k'\sigma'}\hat{c}_{k'\sigma'}\hat{f}_{\sigma'}\hat{f}^{\dagger}_{\sigma'}|0\rangle \\ &+ B^{+-}_{\sigma'\sigma}\langle 0|\hat{c}^{+}_{k_1\sigma}\hat{c}_{k_2\alpha}\hat{f}_{\alpha}\hat{f}^{\dagger}_{\sigma}|0\rangle\langle 0|\hat{c}^{+}_{k'\sigma'}\hat{c}_{k'\sigma'}\hat{f}^{\dagger}_{\sigma'}\hat{f}_{\sigma'}|0\rangle \\ &+ B^{--}_{\sigma\sigma'}\langle 0|\hat{c}^{+}_{k_1\sigma}\hat{c}_{k_2\alpha}\hat{f}_{\alpha}\hat{f}^{\dagger}_{\sigma}|0\rangle\langle 0|\hat{c}^{+}_{k'\sigma'}\hat{c}_{k'\sigma'}\hat{f}_{\sigma'}\hat{f}^{\dagger}_{\sigma'}|0\rangle)],\end{aligned}$$

$$\langle -k\sigma|\hat{H}_{\rm band}|LHB\rangle = \sum_{k'\sigma'}\epsilon_{k'\sigma'}[\delta_{\sigma\sigma'}z_{\sigma}\langle 0|\hat{c}^{+}_{k\sigma}\hat{c}^{+}_{k'\sigma}\hat{c}_{k'\alpha}\hat{f}_{\sigma}|0\rangle + (1-\delta_{\sigma\sigma'})\langle 0|\hat{c}^{+}_{k\alpha}\hat{f}_{\sigma}|0\rangle \times(x_{\sigma'\sigma}\langle 0|\hat{c}^{+}_{k'\sigma'}\hat{c}_{k'\sigma'}\hat{f}^{\dagger}_{\sigma'}\hat{f}_{\sigma'}|0\rangle + v_{\sigma'\sigma}\langle 0|\hat{c}^{+}_{k'\sigma'}\hat{c}_{k'\sigma'}\hat{f}_{\sigma'}\hat{f}^{\dagger}_{\sigma'}|0\rangle)],$$

$$\langle -k\sigma|\hat{H}_{\rm band}|QH\rangle = \sum_{k'\sigma'}\epsilon_{k'\sigma'}[\delta_{\sigma\sigma'}\langle 0|\hat{c}^{+}_{k\sigma}\hat{c}^{+}_{k'\sigma}\hat{c}_{k'\alpha}\hat{f}_{\sigma}|0\rangle + (1-\delta_{\sigma\sigma'})\langle 0|\hat{c}^{+}_{k\alpha}\hat{f}_{\sigma}|0\rangle \times(B^{-+}_{\sigma\sigma'}\langle 0|\hat{c}^{+}_{k'\sigma'}\hat{c}_{k'\sigma'}\hat{f}^{\dagger}_{\sigma'}\hat{f}_{\sigma'}|0\rangle + B^{--}_{\sigma\sigma'}\langle 0|\hat{c}^{+}_{k'\sigma'}\hat{c}_{k'\sigma'}\hat{f}_{\sigma'}\hat{f}^{\dagger}_{\sigma'}|0\rangle)],$$

$$\langle LHB|\hat{H}_{\rm band}|LHB\rangle = \sum_{k'\sigma'}\epsilon_{k'\sigma'}[\delta_{\sigma\sigma'}\langle 0|\hat{f}^{\dagger}_{\sigma}\hat{c}^{+}_{k'\sigma}\hat{c}_{k'\alpha}\hat{f}_{\sigma}|0\rangle + (1-\delta_{\sigma\sigma'})n^{0}_{f\sigma}(B^{++}_{\sigma\sigma'}\langle 0|\hat{c}^{+}_{k'\sigma'}\hat{c}_{k'\sigma'}\hat{f}^{\dagger}_{\sigma'}\hat{f}_{\sigma'} \times|0\rangle + B^{+-}_{\sigma\sigma'}\langle 0|\hat{c}^{+}_{k'\sigma'}\hat{c}_{k'\sigma'}\hat{f}_{\sigma'}\hat{f}^{\dagger}_{\sigma'}|0\rangle) ,$$

$$\langle LHB|\hat{H}_{\rm band}|QH\rangle = \sum_{k'\sigma'}\epsilon_{k'\sigma'}[\delta_{\sigma\sigma'}z_{\sigma}\langle 0|\hat{f}^{\dagger}_{\sigma}\hat{c}^{+}_{k'\sigma}\hat{c}_{k'\alpha}\hat{f}_{\sigma}|0\rangle + (1-\delta_{\sigma\sigma'})n^{0}_{f\sigma}(x_{\sigma'\sigma}\langle 0|\hat{c}^{+}_{k'\sigma'}\hat{c}_{k'\sigma'}\hat{f}^{\dagger}_{\sigma'}\hat{f}_{\sigma'}|0\rangle + v_{\sigma'\sigma}\langle 0|\hat{c}^{+}_{k'\sigma'}\hat{c}_{k'\sigma'}\hat{f}_{\sigma'}\hat{f}^{\dagger}_{\sigma'}|0\rangle) ,$$

$$\langle QH|\hat{H}_{\rm band}|QH\rangle = \sum_{k'\sigma'}\epsilon_{k'\sigma'}[\delta_{\sigma\sigma'}\langle 0|\hat{f}^{\dagger}_{\sigma}\hat{c}^{+}_{k'\sigma}\hat{c}_{k'\alpha}\hat{f}_{\sigma}|0\rangle + (1-\delta_{\sigma\sigma'})n^{0}_{f\sigma}(B^{-+}_{\sigma\sigma'}\langle 0|\hat{c}^{+}_{k'\sigma'}\hat{c}_{k'\sigma'}\hat{f}^{\dagger}_{\sigma'}\hat{f}_{\sigma'}|0\rangle + B^{--}_{\sigma\sigma'}\langle 0|\hat{c}^{+}_{k'\sigma'}\hat{c}_{k'\sigma'}\hat{f}_{\sigma'}\hat{f}^{\dagger}_{\sigma'}|0\rangle)].$$

b. $H_{\rm local}$

Here we define a function for *set*

$$A_{\sigma,\Gamma} = \begin{cases} 1, & \text{if } \sigma \in \Gamma \\ 0, & \text{if } \sigma \notin \Gamma. \end{cases}$$

Then define

$$S_{\Gamma} = E_{\Gamma} + \sum_{\sigma'}\varepsilon_{\sigma'}A_{\sigma',\Gamma}$$

and

$$S_1 = \sum_{\Gamma}E_{\Gamma}m_{\Gamma} + \sum_{\sigma'}\varepsilon_{\sigma'}\sum_{\Gamma\ni\sigma'}m_{\Gamma} = \sum_{\Gamma}m_{\Gamma}S_{\Gamma},$$

$$S_2(\sigma) = \sum_{\Gamma}E_{\Gamma}A_{\sigma,\Gamma}\sqrt{m_{\Gamma}m_{\Gamma\backslash\sigma}} + \sum_{\sigma'}\varepsilon_{\sigma'}\sum_{\Gamma\ni\sigma'}A_{\sigma,\Gamma}\sqrt{m_{\Gamma}m_{\Gamma\backslash\sigma}} = \sum_{\Gamma}A_{\sigma,\Gamma}\sqrt{m_{\Gamma}m_{\Gamma\backslash\sigma}}S_{\Gamma},$$

$$S_3(\sigma) = \sum_{\Gamma}E_{\Gamma}A_{\sigma,\Gamma}m_{\Gamma} + \sum_{\sigma'}\varepsilon_{\sigma'}\sum_{\Gamma\ni\sigma'}A_{\sigma,\Gamma}m_{\Gamma} = \sum_{\Gamma}A_{\sigma,\Gamma}m_{\Gamma}S_{\Gamma},$$

$$S_4(\sigma) = \sum_{\Gamma}E_{\Gamma}A_{\sigma,\Gamma}m_{\Gamma\backslash\sigma} + \sum_{\sigma'}\varepsilon_{\sigma'}\sum_{\Gamma\ni\sigma'}A_{\sigma,\Gamma}m_{\Gamma\backslash\sigma} = \sum_{\Gamma}A_{\sigma,\Gamma}m_{\Gamma\backslash\sigma}S_{\Gamma},$$

$$S_5(\sigma) = \sum_{\Gamma} E_{\Gamma}(1 - A_{\sigma,\Gamma})\sqrt{m_{\Gamma} m_{\Gamma\cup\sigma}} + \sum_{\sigma'} \varepsilon_{\sigma'} \sum_{\Gamma \ni \sigma'} (1 - A_{\sigma,\Gamma})\sqrt{m_{\Gamma} m_{\Gamma\cup\sigma}} = \sum_{\Gamma} (1 - A_{\sigma,\Gamma})\sqrt{m_{\Gamma} m_{\Gamma\cup\sigma}} S_{\Gamma},$$

$$S_6(\sigma) = \sum_{\Gamma} E_{\Gamma}(1 - A_{\sigma,\Gamma}) m_{\Gamma} + \sum_{\sigma'} \varepsilon_{\sigma'} \sum_{\Gamma \ni \sigma'} (1 - A_{\sigma,\Gamma}) m_{\Gamma} = \sum_{\Gamma} (1 - A_{\sigma,\Gamma}) m_{\Gamma} S_{\Gamma},$$

$$S_7(\sigma) = \sum_{\Gamma} E_{\Gamma}(1 - A_{\sigma,\Gamma}) m_{\Gamma\cup\sigma} + \sum_{\sigma'} \varepsilon_{\sigma'} \sum_{\Gamma \ni \sigma'} (1 - A_{\sigma,\Gamma}) m_{\Gamma\cup\sigma} = \sum_{\Gamma} (1 - A_{\sigma,\Gamma}) m_{\Gamma\cup\sigma} S_{\Gamma},$$

$$S_{25}(\sigma) = \sum_{\Gamma} E_{\Gamma}\left[A_{\sigma,\Gamma} \frac{m_{\Gamma}}{n^0_{f\sigma}} - (1 - A_{\sigma,\Gamma}) \frac{m_{\Gamma}}{1 - n^0_{f\sigma}} \right] + \sum_{\sigma'} \varepsilon_{\sigma'} \sum_{\Gamma \ni \sigma'} A_{\sigma',\Gamma} \left[A_{\sigma,\Gamma} \frac{m_{\Gamma}}{n^0_{f\sigma}} - (1 - A_{\sigma,\Gamma}) \frac{m_{\Gamma}}{1 - n^0_{f\sigma}} \right] = \left[A_{\sigma,\Gamma} \frac{m_{\Gamma}}{n^0_{f\sigma}} - (1 - A_{\sigma,\Gamma}) \frac{m_{\Gamma}}{1 - n^0_{f\sigma}} \right] S_{\Gamma}.$$

Thus

$$\langle + k_1\sigma|\hat{H}_{\text{local}}|+ k_2\sigma\rangle = \langle 0|\hat{c}_{k_1\sigma}\hat{c}^{+}_{k_2\sigma}|0\rangle S_1 + \langle 0|\hat{c}_{k_1\sigma}\hat{f}^{\dagger}_{\sigma}|0\rangle \times \langle 0|\hat{f}_{\sigma}\hat{c}^{+}_{k_2\sigma}|0\rangle S_{25}(\sigma),$$

$$\langle + k\sigma|\hat{H}_{\text{local}}|UHB\rangle = \frac{1}{\sqrt{n^0_{f\sigma}(1 - n^0_{f\sigma})}} \langle 0|\hat{c}_{k\sigma}\hat{f}^{\dagger}_{\sigma}|0\rangle S_2(\sigma),$$

$$\langle + k\sigma|\hat{H}_{\text{local}}|QE\rangle = \frac{1}{n^0_{f\sigma}} \langle 0|\hat{c}_{k\sigma}\hat{f}^{\dagger}_{\sigma}|0\rangle S_3(\sigma),$$

$$\langle UHB|\hat{H}_{\text{local}}|UHB\rangle = S_4(\sigma),$$

$$\langle UHB|\hat{H}_{\text{local}}|QE\rangle = \frac{\sqrt{1 - n^0_{f\sigma}}}{\sqrt{n^0_{f\sigma}}} S_2(\sigma),$$

$$\langle QE|\hat{H}_{\text{local}}|QE\rangle = \frac{1 - n^0_{f\sigma}}{n^0_{f\sigma}} S_3(\sigma),$$

$$\langle - k_1\sigma|\hat{H}_{\text{local}}|- k_2\sigma\rangle = \langle 0|\hat{c}^{+}_{k_1\sigma}\hat{c}_{k_2\sigma}|0\rangle S_1 - \langle 0|\hat{c}^{+}_{k_1\sigma}\hat{f}_{\sigma}|0\rangle \times \langle 0|\hat{f}^{\dagger}_{\sigma}\hat{c}_{k_2\sigma}|0\rangle S_{25}(\sigma),$$

$$\langle - k\sigma|\hat{H}_{\text{local}}|LHB\rangle = \frac{1}{\sqrt{n^0_{f\sigma}(1 - n^0_{f\sigma})}} \langle 0|\hat{c}^{+}_{k\sigma}\hat{f}_{\sigma}|0\rangle S_5(\sigma),$$

$$\langle - k\sigma|\hat{H}_{\text{local}}|QH\rangle = \frac{1}{1 - n^0_{f\sigma}} \langle 0|\hat{c}^{+}_{k\sigma}\hat{f}_{\sigma}|0\rangle S_6(\sigma),$$

$$\langle LHB|\hat{H}_{\text{local}}|LHB\rangle = S_7(\sigma),$$

$$\langle LHB|\hat{H}_{\text{local}}|QH\rangle = \frac{\sqrt{n^0_{f\sigma}}}{\sqrt{1 - n^0_{f\sigma}}} S_5(\sigma),$$

$$\langle QH|\hat{H}_{\text{local}}|QH\rangle = \frac{n^0_{f\sigma}}{1 - n^0_{f\sigma}} S_6(\sigma).$$

c. H_V

$$\langle + k_1\sigma|\hat{H}_V|+ k_2\sigma\rangle = \sum_{k'\sigma'} V_{k'\sigma'}[\delta_{\sigma\sigma'} z_{\sigma}(\langle 0|\hat{c}_{k_1\sigma}\hat{c}^{+}_{k'\sigma}\hat{f}_{\sigma}\hat{c}^{+}_{k_2\sigma}|0\rangle + \langle 0|\hat{c}_{k_1\sigma}\hat{f}^{\dagger}_{\sigma}\hat{c}_{k'\sigma}\hat{c}^{+}_{k_2\sigma}|0\rangle) + (1 - \delta_{\sigma\sigma'}) \times (\langle 0|\hat{c}^{+}_{k'\sigma'}\hat{f}_{\sigma'}|0\rangle + \langle 0|\hat{f}^{\dagger}_{\sigma'}\hat{c}_{k'\sigma'}|0\rangle) \times (x_{\sigma\sigma'}\langle 0|\hat{c}_{k_1\sigma}\hat{c}^{+}_{k_2\sigma}\hat{f}^{\dagger}_{\sigma}\hat{f}_{\sigma}|0\rangle + v_{\sigma\sigma'}\langle 0|\hat{c}_{k_1\sigma}\hat{c}^{+}_{k_2\sigma}\hat{f}_{\sigma}\hat{f}^{\dagger}_{\sigma}|0\rangle)],$$

$$\langle + k\sigma|\hat{H}_V|UHB\rangle = \sum_{k'\sigma'} V_{k'\sigma'}[\delta_{\sigma\sigma'}\langle 0|\hat{c}_{k\sigma}\hat{c}^{+}_{k'\sigma}\hat{f}_{\sigma}\hat{f}^{\dagger}_{\sigma}|0\rangle + (1 - \delta_{\sigma\sigma'})\langle 0|\hat{c}_{k\sigma}\hat{f}^{\dagger}_{\sigma}|0\rangle(y_{\sigma\sigma'}\langle 0|\hat{c}^{+}_{k'\sigma'}\hat{f}_{\sigma'}|0\rangle + w_{\sigma\sigma'}\langle 0|\hat{f}^{\dagger}_{\sigma'}\hat{c}_{k'\sigma'}|0\rangle)],$$

$$\langle + k\sigma|\hat{H}_V|QE\rangle = \sum_{k'\sigma'} V_{k'\sigma'}[\delta_{\sigma\sigma'} z_{\sigma}\langle 0|\hat{c}_{k\sigma}\hat{c}^{+}_{k'\sigma}\hat{f}_{\sigma}\hat{f}^{\dagger}_{\sigma}|0\rangle + + (1 - \delta_{\sigma\sigma'}) x_{\sigma\sigma'}\langle 0|c_{k\sigma}f^{\dagger}_{\sigma}|0\rangle(\langle 0|c^{+}_{k'\sigma'}f_{\sigma'}|0\rangle + \langle 0|f^{\dagger}_{\sigma'}c_{k'\sigma'}|0\rangle)],$$

$$\langle UHB|\hat{H}_V|UHB\rangle = \sum_{k'\sigma'} V_{k'\sigma'}(1 - \delta_{\sigma\sigma'}) v_{\sigma\sigma'}(1 - n^0_{f\sigma}) \times (\langle 0|\hat{c}^{+}_{k'\sigma'}\hat{f}_{\sigma'}|0\rangle + \langle 0|\hat{f}^{\dagger}_{\sigma'}\hat{c}_{k'\sigma'}|0\rangle),$$

$$\langle UHB|\hat{H}_V|QE\rangle = \sum_{k'\sigma'} V_{k'\sigma'}(1 - \delta_{\sigma\sigma'})(1 - n^0_{f\sigma}) \times (w_{\sigma\sigma'}\langle 0|c^{+}_{k'\sigma'}f_{\sigma'}|0\rangle + y_{\sigma\sigma'}\langle 0|f^{\dagger}_{\sigma'}c_{k'\sigma'}|0\rangle),$$

$$\langle QE|H_V|QE\rangle = \sum_{k'\sigma'} V_{k'\sigma'}(1 - \delta_{\sigma\sigma'}) x_{\sigma\sigma'}(1 - n^0_{f\sigma}) \times (\langle 0|c^{+}_{k'\sigma'}f_{\sigma'}|0\rangle + \langle 0|f^{\dagger}_{\sigma'}c_{k'\sigma'}|0\rangle),$$

$$\langle -k_1\sigma|\hat{H}_V|-k_2\sigma\rangle = \sum_{k'\sigma'} V_{k'\sigma'}[\delta_{\sigma\sigma'} z_\sigma(\langle 0|\hat{c}^+_{k_1\sigma}\hat{c}^+_{k'\sigma}\hat{f}_\sigma\hat{c}_{k_2\sigma}|0\rangle + \langle 0|\hat{c}^+_{k_1\sigma}\hat{f}^\dagger_\sigma\hat{c}_{k'\sigma}\hat{c}_{k_2\sigma}|0\rangle) + (1-\delta_{\sigma\sigma'}) \times(\langle 0|\hat{c}^+_{k'\sigma'}\hat{f}_{\sigma'}|0\rangle + \langle 0|\hat{f}^\dagger_{\sigma'}\hat{c}_{k'\sigma'}|0\rangle) \times(x_{\sigma\sigma'}\langle 0|\hat{c}^+_{k_1\sigma}\hat{c}_{k_2\sigma}\hat{f}^\dagger_\sigma\hat{f}_\sigma|0\rangle + v_{\sigma\sigma'}\langle 0|\hat{c}^+_{k_1\sigma}\hat{c}_{k_2\sigma}\hat{f}_\sigma\hat{f}^\dagger_\sigma|0\rangle)],$$

$$\langle -k\sigma|\hat{H}_V|LHB\rangle = \sum_{k'\sigma'} V_{k'\sigma'}[\delta_{\sigma\sigma'}\langle 0|\hat{c}^+_{k\sigma}\hat{f}^\dagger_\sigma\hat{c}_{k'\sigma}\hat{f}_\sigma|0\rangle + (1-\delta_{\sigma\sigma'}) \times\langle 0|\hat{c}^+_{k\sigma}\hat{f}_\sigma|0\rangle(w_{\sigma\sigma'}\langle 0|\hat{c}^+_{k'\sigma'}\hat{f}_{\sigma'}|0\rangle + y_{\sigma\sigma'}\langle 0|\hat{f}^\dagger_{\sigma'}\hat{c}_{k'\sigma'}|0\rangle)],$$

$$\langle -k\sigma|H_V|QH\rangle = \sum_{k'\sigma'} V_{k'\sigma'}[\delta_{\sigma\sigma'} z_\sigma\langle 0|c^+_{k\sigma}f^\dagger_\sigma c_{k'\sigma}f_\sigma|0\rangle + (1-\delta_{\sigma\sigma'})v_{\sigma\sigma'}\langle 0|c^+_{k\sigma}f_\sigma|0\rangle(\langle 0|c^+_{k'\sigma'}f_{\sigma'}|0\rangle + \langle 0|f^\dagger_{\sigma'}c_{k'\sigma'}|0\rangle)],$$

$$\langle LHB|\hat{H}_V|LHB\rangle = \sum_{k'\sigma'} V_{k'\sigma'}(1-\delta_{\sigma\sigma'})x_{\sigma\sigma'}n^0_{f\sigma} \times(\langle 0|\hat{c}^+_{k'\sigma'}\hat{f}_{\sigma'}|0\rangle + \langle 0|\hat{f}^\dagger_{\sigma'}\hat{c}_{k'\sigma'}|0\rangle),$$

$$\langle LHB|H_V|QH\rangle = \sum_{k'\sigma'} V_{k'\sigma'}(1-\delta_{\sigma\sigma'})n^0_{f\sigma}(y_{\sigma\sigma'}\langle 0|c^+_{k'\sigma'}f_{\sigma'}|0\rangle + w_{\sigma\sigma'}\langle 0|f^\dagger_{\sigma'}c_{k'\sigma'}|0\rangle),$$

$$\langle QH|H_V|QH\rangle = \sum_{k'\sigma'} V_{k'\sigma'}(1-\delta_{\sigma\sigma'})v_{\sigma\sigma'}n^0_{f\sigma} \times(\langle 0|c^+_{k'\sigma'}f_{\sigma'}|0\rangle + \langle 0|f^\dagger_{\sigma'}c_{k'\sigma'}|0\rangle),$$

[1] P. Hohenberg and W. Kohn, Phys. Rev. **136** B864 (1964); W. Kohn and L. J. Sham, *ibid.* **140**, A1133 (1965).
[2] V. I. Anisimov, J. Zaanen, and O. K. Andersen, Phys. Rev. B **44**, 943 (1991).
[3] V. I. Anisimov, F. Aryasetiawan, and A. I. Lichtensten, J. Phys.: Condens. Matter **9**, 767 (1997).
[4] N. F. Mott, Proc. Phys. Soc., London, Sect. A **62**, 416 (1949).
[5] N. F. Mott, Can. J. Phys. **34**, 1356 (1956).
[6] N. F. Mott, Philos. Mag. **6**, 287 (1961).
[7] M. C. Gutzwiller, Phys. Rev. **137**, A1726 (1965).
[8] D. Vollhardt, Rev. Mod. Phys. **56**, 99 (1984).
[9] J. Bünemann, W. Weber, and F. Gebhard, Phys. Rev. B **57**, 6896 (1998).
[10] X. Deng, X. Dai, and Z. Fang, EPL **83**, 37008 (2008).
[11] X. Deng, L. Wang, X. Dai, and Z. Fang, Phys. Rev. B **79**, 075114 (2009).
[12] A. Georges, G. Kotliar, W. Krauth, and M. J. Rozenberg, Rev. Mod. Phys. **68**, 13 (1996).
[13] N. F. Mott, *Metal Insulator Transitions* (Taylor & Francis, London, 1990).
[14] N. Tsuda, K. Nasu, A. Yanase, and K. Siratori, *Electronic Conduction in Oxides, Springer Series in Solid State Sciences* (Springer-Verlag, Berlin, 1991), Vol. 94.
[15] S. S. Kancharla and E. Dagotto, Phys. Rev. Lett. **98**, 016402 (2007).
[16] Q. Si, S. Rabello, K. Ingersent, and J. Lleweilun Smithm, Nature (London) **413**, 804 (2001).
[17] P. Gegenwart, Q. Si, and F. Steglich, Nat. Phys. **4**, 186 (2008).
[18] V. I. Anisimov, A. I. Poteryaev, M. A. Korotin, A. O. Anokhin, and G. Kotliar, J. Phys.: Condens. Matter **9**, 7359 (1997).
[19] X. Dai, S. Y. Savrasov, G. Kotliar, A. Migliori, H. Ledbetter, and E. Abrahams, Science **300**, 953 (2003).
[20] J. H. Shim, K. Haule, G. Kotliar, Phys. Rev. B **79**, 060501 (2009).
[21] G. Kotliar, S. Y. Savrasov, K. Haule, V. S. Oudovenko, O. Parcollet, and C. A. Marianetti, Rev. Mod. Phys. **78**, 865 (2006).
[22] K. Held, Adv. Phys. **56**, 829 (2007).
[23] H. O. Jeschke and G. Kotliar, Phys. Rev. B **71**, 085103 (2005).
[24] S. Y. Savrasov, V. Oudovenko, K. Haule, D. Villani, and G. Kotliar, Phys. Rev. B **71**, 115117 (2005).
[25] M. J. Han, X. Wan, and S. Y. Savrasov, Phys. Rev. B **78**, 060401(R) (2008).
[26] M. J. Rozenberg, G. Kotliar, and X. Y. Zhang, Phys. Rev. B **49**, 10181 (1994).
[27] S. Y. Savrasov, V. Oudovenko, K. Haule, D. Villani, and G. Kotliar, Phys. Rev. B **71**, 115117 (2005).
[28] M. Jarrell and Th. Pruschke, Phys. Rev. B **49**, 1458 (1994); K. Haule, V. Oudovenko, S. Y. Savrasov, and G. Kotliar, Phys. Rev. Lett. **94**, 036401 (2005).
[29] L. Chioncel, L. Vitos, I. A. Abrikosov, J. Kollar, M. I. Katsnelson, and A. I. Lichtenstein, Phys. Rev. B **67**, 235106 (2003); V. Drchal, V. Janiš, J. Kudrnovsk, V. S. Oudovenko, X. Dai, K. Haule, and G. Kotliar, J. Phys. Condens. Matter **17**, 61 (2005).
[30] Michel Caffarel and Werner Krauth, Phys. Rev. Lett. **72**, 1545 (1994).
[31] L. Laloux, A. Georges, and W. Krauth, Phys. Rev. B **50**, 3092 (1994).
[32] J. E. Hirsch and R. M. Fye, Phys. Rev. Lett. **56**, 2521 (1986).
[33] R. Bulla, A. C. Hewson, and Th. Pruschke, J. Phys.: Condens. Matter **10**, 8365 (1998).
[34] P. Werner, A. Comanac, L. de' Medici, M. Troyer, and A. J. Millis, Phys. Rev. Lett. **97**, 076405 (2006).

[35] A. N. Rubtsov, V. V. Savkin, and A. I. Lichtenstein, Phys. Rev. B **72**, 035122 (2005).
[36] X. Dai, S. Y. Savrasov, G. Kotliar, A. Migliori, H. Ledbetter, and E. Abrahams, Science **300**, 953 (2003).
[37] K. Haule, J. H. Shim, and G. Kotliar, Phys. Rev. Lett. **100**, 226402 (2008).
[38] T. M. Rice and K. Ueda, Phys. Rev. B **34**, 6420 (1986).
[39] H. Shiba and P. Fazekas, Prog. Theor. Phys. **101**, 403 (1990).
[40] F. Tan and Q.-H. Wang, Phys. Rev. Lett. **100**, 117004 (2008).
[41] X. Dai, G. Kotliar, and Z. Fang, arXiv:cond-mat/0611075 (unpublished).
[42] A. L. Fetter and J. D. Walecka, *Quantum Theory of Many-Particle Systems* (McGraw-Hill, New York, 1971).
[43] O. Gunnarsson and K. Schönhammer, Phys. Rev. B **28**, 4315 (1983).
[44] A. C. Hewson, *The Kondo Problem to Heavy Fermions* (Cambridge University Press, Cambridge, 1993).
[45] S. Sugano, Y. Tanabe, and H. Kamimura, *Multiplets of Transition-Metal Ions in Crystals, Pure and Applied Physics* (Academic, New York, 1970), Vol. 33.
[46] Kensuke Inaba and Akihisa Koga, Phys. Rev. B **73**, 155106 (2006).
[47] A. Koga, N. Kawakami, T. M. Rice, and M. Sigrist, Phys. Rev. Lett. **92**, 216402 (2004).
[48] L. de'Medici, A. Georges, and S. Biermann, Phys. Rev. B **72**, 205124 (2005).
[49] Yoshiaki Ono, Ralf Bullab, and Michael Potthoff, Physica B **329-333**, 942 (2003).